AUTOMATIC CLASSIFICATION OF GLAUCOMATIC PATIENTS BASED ON VESSEL SHAPE ANALYSIS

P.A. Asvestas*, K.K. Delibasis*, N.A. Mouravliansky*, G.K. Matsopoulos* and T. Zeyen **

* Institute of Communication and Computer Systems, 9 Iroon Polytechneiou str., 15780, Athens, Greece
** Universiteit Antwerpen (UIA); Dienst Oogheelkunde - Middelheim Hospitaal, Lindendreef 1 B-2020 Antwerpen, Belgium

gmatso@esd.ece.ntua.gr

Abstract: Glaucoma, a leading cause of blindness worldwide, is a progressive optic neuropathy with characteristic structural changes in the optic nerve head reflected in the visual field. Even though a number of variables, including visual field defects, have been used by the experts in order to identify early glaucomatous damage, there is a need for computer-based methods that can detect glaucomatous damages at early stages so that treatment to prevent further progression can be instigated. The paper is mainly focused on the description of a methodology based on image processing techniques for the estimation of quantitative parameters to define vessel deformation in order to assist early detection of glaucoma.

Introduction

Glaucoma is a disease of the eye that is mainly associated with an increase in intraocular pressure. A build-up of fluid within the eye eventually leads to damage in the optic nerve fibers and a gradual loss of a patient's visual field. Diagnosis may be based on a combination of parameters [1] and [2], but the most dependable single index is probably the identification of a characteristic pattern of visual field defects. There have been numerous studies towards the quantification of parameters that can be used for the discrimination of normal against glaucomatous retinal data using computerized systems [3]-[5].

The purpose of this work is to extract attributes from retinal images with diagnostic information capable for automatic identification of glaucomatic patients, without additional information concerning the patient. This work is based on the theory that increased endophthalmiac pressure damages the fibrous and nervous tissue at the basis of the retina, inside the optic disk, therefore causing the attached retinal vessels to deform, with a possible preferable direction towards the periphery of the disk. The method utilizes the shape deformation that occurs in vessels during the progression of the disease to train a classifier to classify vessels and in extension to assist early detection of glaucoma.

Materials and Methods

A number of glaucomatic patients and non-glaucomatic subjects were imaged with a fundus camera at regular intervals of six months. The first image serves as the reference image (baseline). Corresponding vessel segments between the reference image and subsequent images are compared by means of shape descriptors and classified as glaucomatic or not.

The system consists of the following software components:

- Preprocessing which involves extraction of vessel centerlines and bifurcation points.
- Registration using Self-Organizing Maps.
- Calculation of retinal vessel attributes.
- Feature selection.
- Classification.

I. Retinal image preprocessing

The vessel centerlines are detected by means of differential geometry, as follows: for a gray level retinal image $I(x,y)$, the centerlines of vessels that are brighter than the surrounding background consist of the ridge points of the surface $S=\{(x,y,I(x,y))\}$.

The detection of the ridge points can be accomplished using the following methodology: Firstly, the second derivatives, $I_{xx}(x_0,y_0)$, $I_{xy}(x_0,y_0)$ and $I_{yy}(x_0,y_0)$, of the image w.r.t x and y at each pixel position (x_0,y_0) are estimated by convolving the image with the appropriate 2D Gaussian kernels. Then, the eigenvalues and eigenvectors of the Hessian matrix:

$$\mathbf{H}(x_0,y_0)=\begin{bmatrix} I_{xx}(x_0,y_0) & I_{xy}(x_0,y_0) \\ I_{xy}(x_0,y_0) & I_{yy}(x_0,y_0) \end{bmatrix} \qquad (1)$$

are calculated using the Jacobi method. Let $\mathbf{u}=(u_x,u_y)$, $u_x^2+u_y^2=1$, be the eigenvector corresponding to the eigenvalue of maximum negative value. Then, the point (x_0,y_0) is a ridge point if the

ISSN: 1727-1983

first directional derivative across the direction of $\mathbf{u}$ at (x_0, y_0) vanishes, namely

$$\left\langle \nabla I(x_0, y_0), \mathbf{u} \right\rangle = 0 \tag{2}$$

where $\langle\ \rangle$ denotes the inner product.
It can be shown [6] that if the following relation holds:

$$(tu_x, tu_y) \in [-0.5, 0.5] \times [-0.5, 0.5] \tag{3}$$

where

$$t = -\frac{u_x I_x(x_0, y_0) + u_y I_y(x_0, y_0)}{u_x^2 I_{xx}(x_0, y_0) + 2u_x u_y I_{xy}(x_0, y_0) + u_y^2 I_{yy}(x_0, y_0)} \tag{4}$$

and I_x, I_y are the first derivatives of I w.r.t x and y, then the pixel (x_0, y_0) is marked as a ridge pixel with exact position $(x_0 + tu_x, y_0 + tu_y)$.

A pixel that belongs to two vessels at the same time is defined as a bifurcation pixel. Fig. 1 shows an example of bifurcation point extraction according the preprocessing step.

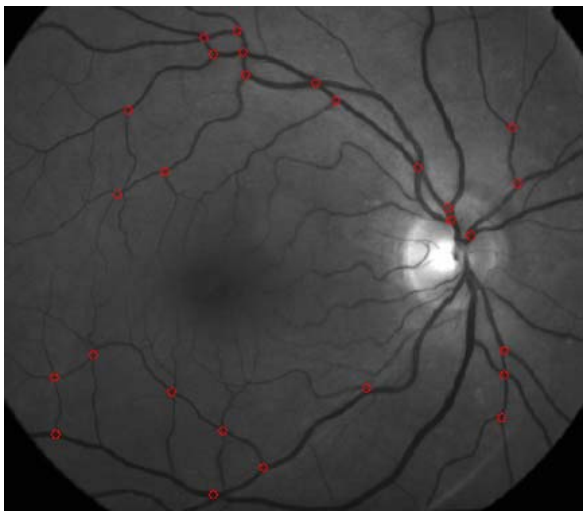

Figure 1: Example of bifurcation point extraction according to the preprocessing step.

II. Automatic retinal image registration

This step is necessary for automatic vessel segment selection. Aligned vessels define corresponding endpoints, so that vessel shape descriptor calculation can be done in a meaningful way. The method is outlined as following [6]: Let I_R be the reference image and I_F the image to be registered. The bifurcation points of the reference retinal image are extracted according to the preprocessing step. A self organizing map (SOM) is used to extract the affine transformation parameters, according to the following method:

A SOM is constructed by assigning one neuron to each bifurcation point $\mathbf{P}_i = (x_i, y_i)$, $i = 1, \ldots, N$, of the reference image, where N is the number of the bifurcation points detected in the reference image. A weight vector $\mathbf{w}_i = (dx_i, dy_i, \theta_i)$, which holds the parameters of a local rigid transformation, is assigned to each neuron, where dx_i, dy_i, θ_i are the horizontal, vertical displacement and the angle of rotation, respectively. Additionally, each neuron is assigned a square area $A_i = [x_i - R, x_i + R] \times [y_i - R, y_i + R]$. In this application R is set to 19.
Let $\mu_A(I)$ be the restriction operator of the image I to a region $A \subset \Re^2$ and $T_{\mathbf{w}}(A) \subset \Re^2$ be the rigid transformation operator with parameters defined by the vector $\mathbf{w}$ applied on a region A. Furthermore $MoM(I_1, I_2)$ denotes a measure of match (MoM) between the spatial coincidence of two images I_1 and I_2. The MoM was the gradient difference defined as following [7]:

$$MoM(I_1, I_2) = \sum_{x,y} \frac{1}{1 + \left[I_{1x}(x,y) - I_{2x}(x,y) \right]^2} + \sum_{x,y} \frac{1}{1 + \left[I_{1y}(x,y) - I_{2y}(x,y) \right]^2} \tag{5}$$

where the subscript x (y) denotes the partial derivative of the image w.r.t x (y).

The SOM network is initialized as follows: the iteration number n is set to 0. For each neuron i, the weight vector is set to zero values, $\mathbf{w}_i(0) = (0,0,0)$, the quantity $MoM_i(0) = MoM\left(\mu_A(I_1), \mu_{T_{\mathbf{wi}(0)}(A_i)}(I_2)\right)$ is calculated, the variable MoM_{best} is set to a very large (in magnitude) negative value and the iteration variable, n, is set to 1.
The SOM network is trained as follows:

- While n is less than the maximum number of iterations, $n_{\max}$, do:
  - If the average value of the MoM of neurons of iteration n-1, $MoM_{ave}(n-1)$, is better than MoM_{best} then $MoM_{best} = MoM_{ave}(n-1)$ and the current weights are stored in $\mathbf{w}_i$.
  - An input signal, $\mathbf{s}(n) = (dx(n), dy(n), \theta(n))$, is generated randomly, using the following random number generator:

$$s_j(n) = w_{k_n, j} + \operatorname{sgn}(v_j - 0.5) TM(n) \times \left[\left(1 + \frac{1}{TM(n)} \right)^{|2v_j - 1|} - 1 \right] (U_j - L_j) \tag{6}$$

ISSN: 1727-1983

where $j = 1,2,3$, $s_j(n)$ denotes the jth-component of the vector $\mathbf{s}(n)$, U_j and L_j are the upper and lower limits for the parameters, v_j is a uniformly distributed random variable in the range $[0,1]$, n the iteration number and $TM(n)$ is defined as:

$$TM(n) = \begin{cases} 1, & n = 0 \\ \exp\left(-2\left(q(n)\right)^{1/n}\right), & n > 0 \end{cases} \quad (7)$$

- For every neuron, the quantity $MoM_i(n) = MoM\left(\mu_{A_i}(I_R), \mu_{T_{s(n)}(A_i)}(I_F)\right)$ is calculated.
- The winning neuron k_n in the current iteration n is defined by:

$$k_n = \arg\max_i \left\{MoM_i(n)\right\} \quad (8)$$

under the condition $MoM_{k_n}(n) > MoM_{ave}(n)$.

- The weights of the neurons are updated according to the following equation:

$$\mathbf{w}_i(n) = \mathbf{w}_i(n-1) + h(k_n, n, i)\left[\mathbf{s}(n) - \mathbf{w}(n)\right] \quad (9)$$

where

$$h(k_n, n, i) = \begin{cases} L^{q(n)}, & \left\|\mathbf{P}_{k_n} - \mathbf{P}_i\right\| < \alpha^{q(n)} d_0 \\ 0, & \text{otherwise} \end{cases},$$

$q(n) = \left\lfloor \frac{n}{p+1} \right\rfloor$, $\lfloor\ \rfloor$ denotes the floor operator, d_0 provides the initial radius of circular region of influence around the winning neuron, whereas the radius of the region is being reduced with iteration number with a rate defined by α which was set to 0.995. Typical values for L fall within the [0.99, 1.0] range and p is set to 200.

- $n = n + 1$

Fig. 2(a) and 2(b) show a pair of retinal images before registration. The result of the proposed registration scheme is displayed in Fig. 3(c), where the vessel centerlines of the reference image are superimposed on the transformed image.

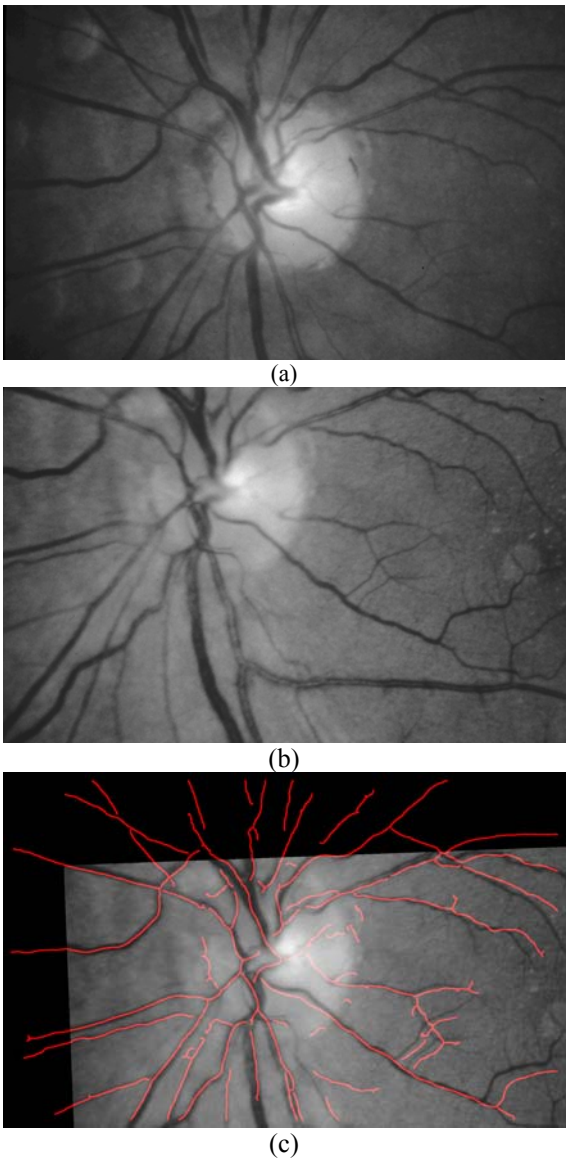

(a) (b) (c)

Figure 2. (a) Reference image. (b) Image to be registered. (c) Superposition of reference vessel centerlines on the transformed image.

III. Calculation of retinal vessel attributes

If we assume that a vessel is a parametric curve $r(k) = \{x(k), y(k)\}$, $k = 0,1,\ldots,K-1$, then the quantity $c(k) = \sqrt{\left(x(k) - x_c\right)^2 + \left(y(k) - y_c\right)^2}$ is readily available, where (x_c, y_c) is the vessel's center of mass. The signal $c(k)$ is back traced and interpolated to 1024 points, producing $d(k)$. Finally, the discrete Wavelet Transform (DWT) is applied to the signal, described as follows:

ISSN: 1727-1983

$$L_j^{(0)} = d(j)$$
$$L_j^{(m)} = \sum_k g(2j-k) L_j^{(m-1)}, \quad m = 1,2,\ldots \qquad (10)$$
$$D_j^{(m)} = \sum_k h(2j-k) L_j^{(m-1)}$$

where $g(k)$, $h(k)$ are quadrature mirror filters, $L_j^{(m)}$, $D_j^{(m)}$ are the approximation and detail coefficients, respectively and m is the decomposition level. The representation of the signal using the Wavelet Transform is done by the wavelet coefficients, up to depth M :

$$\left\{ L_j^{(M)}, \left\{ D_j^{(m)} \right\} \quad 1 \le m \le M \right\} \qquad (11)$$

Finally, vessel signal approximation of the first level and the detail coefficients up to the third level of decomposition are obtained to serve as vessel shape descriptors.

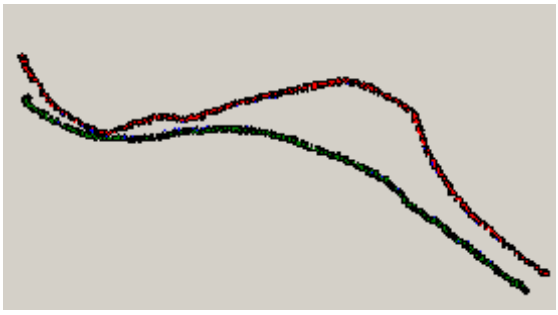

Figure 3. Two corresponding vessels from the baseline image and the first image after glaucoma diagnosis. The change of the vessel shape is evident.

IV. Patient Classification

The purpose of this step is to utilize the vessel attributes defined above to achieve correct classification of vessels / patients to glaucomatic / non-glaucomatic. The relative change of the logarithm of the magnitude of the wavelet coefficients of the retinal vessels between the reference and the second image are used as attributes.

In theory, the feature selection process is a selection of a subset of attributes from a set of available attributes, that will optimize the classification process, in terms of a) Accuracy of classification function, b) Training time, c) Size of training set and d) Computational cost of executing the classification.

Due to the high number of vessel attributes, it became necessary to eliminate attributes, which are linearly correlated or carry no diagnostic information. Therefore, the sequential float forward search (SFFS) technique was employed, which can be formulated according to [8].

The algorithm is described in pseudocode as follows:

Let D be the number of available features, i ($1 \le i \le D$) denotes a feature, X_k is a subset of features containing k features and J is an evaluation function.

- $X_0 = \varnothing$ *and* $k = 0$.
- *While* $k < D$
  - *Find the most significant feature:* $y = \arg\max_{a \in Y - X_k} J(X_k \cup \{a\})$
  - $X_{k+1} = X_k \cup y$
  - $k = k + 1$
  - *Find the least significant feature:* $x = \arg\max_{a \in X_k} J(X_k - a)$
  - *While* $J(X_k - \{x\}) > J(X_{k-1})$
    - $X_{k-1} = X_k - \{x\}$
    - $k = k - 1$
    - *Find the least significant feature:* $x = \arg\max_{a \in X_k} J(X_k - a)$
    - *End*
  - *End*

The best feature set, X^*, is obtained by means of the following rule:

$$X^* = X_{k^*}$$
$$k^* = \arg\min_k \left\{ J(X_k) = J_{\max} \right\} \qquad (12)$$
$$J_{\max} = \max_k \left\{ J(X_k) \right\}$$

In this specific implementation, the classification rate of the fuzzy C-means clustering algorithm was employed as the evaluation function J [9]. According to the fuzzy clustering, each point does not pertain to a given cluster, but has a degree of belonging to a certain cluster, as in fuzzy logic. For each point $\mathbf{x}$, there is a coefficient giving the degree of being in the kth cluster, $u_k(\mathbf{x})$. Usually, the sum of those coefficients has to be one, so that $u_k(\mathbf{x})$ denotes a probability of belonging to a certain cluster:

$$\forall \mathbf{x} \sum_{k=1}^{num\,clusters} u_k(\mathbf{x}) = 1 \qquad (13)$$

With fuzzy c-means, the centroid of a cluster is computed as being the mean of all points, weighted by their degree of belonging to the cluster, that is:

$$\mathbf{c}_k = \frac{\sum_{\mathbf{x}} u_k(\mathbf{x}) \mathbf{x}}{\sum_{\mathbf{x}} u_k(\mathbf{x})} \qquad (14)$$

The degree of being in a certain cluster is the inverse of the distance to the cluster. Then, the coefficients are normalized and fuzzyfied with a real parameter m > 1 so that their sum is 1:

ISSN: 1727-1983

$$u_k(\mathbf{x}) = \frac{1}{\sum_j \left[\frac{\|\mathbf{c}_k(\mathbf{x}) - \mathbf{x}\|}{\|\mathbf{c}_j(\mathbf{x}) - \mathbf{x}\|} \right]^{\frac{1}{m-1}}} \quad (15)$$

Results

Images from 23 non-glaucomatic subjects and 26 glaucomatic patients were used as a test set in this study. 44 pairs of vessels were obtained from the non-glaucomatic group and 42 pairs from the gluacomatic group. The classification was performed by means of the fuzzy C-means algorithm.

Effort has been made by skilled physicians to identify multiple vessel pairs, to enhance the train and test process.

A subject was assigned to the non-glaucomatic group (NGG) if all vessel pairs were found not glaucomatic, otherwise the subject was assigned to the glaucomatic group (GG). Table 1 presents the results for the final patient classification.

Table 1: Classification results

	Vessels		**Patients**	
	NGG	GG	NGG	GG
Correct Classif/Total number	30/33	25/36	17/23	22/26
Classif. Rate (%)			73.9	84.6

The details of the results at vessel level for both classes are given in the two following tables. Correct classification for vessel and patient is marked by "√", whereas incorrect classification is marked by "X".

Table 2 Classification results for glaucomatic patients.

Pat. No	**1**	**2**	**3**	**Patient classification**
1	√	√		√
2	√			√
3	√	√	√	√
4	√	√		√
5	√	√		√
6	√	√		√
7	√			√
8	√			√
9	X	X		X
10	√			√
11	X			X
12	√			√
13	√			√
14	X	X		X
15	√	√		√
16	√			√
17	X			X
18	√	√	√	√
19	√	√		√
20	√		√	√
21	√			√
22	√	X		√
23	√			√
24	√	√	√	√
25	√			√
26	√			√

Table 3 Classification results for non-glaucomatic subjects.

Pat. No	**1**	**2**	**3**	**Patient Classification**
1	√	√		√
2	√	X	√	X
3	√	√		√
4	√	√		√
5	√	√		√
6	√	X		X
7	√	√		√
8	√			√
9	√	√		√
10	√	√		√
11	√	√		√
12	√	√		√
13	√	X		X
14	√	√		√
15	√	√		√
16	X	X		X
17	√	X		X
18	√	√		√
19	√	√		√
20	√	X		X
21	√	√		√
22	√			√
23	√			√

Discussion

In this paper, a new methodology for identifying shape changes of retinal vessels that are due to the presence of glaucoma is developed. The methodology is based on the comparison of corresponding vessel segments by means of the discrete wavelet transform. The total classification rate obtained by the proposed methodology is calculated equal to 79.6%.

Within the group of subjects that was investigated, the percentage change of the wavelet coefficients was lower in the vessels obtained from the non-glaucomatic subjects compared to the glaucomatic patients. This

ISSN: 1727-1983

finding shows that glaucoma may induce deformation of retinal vessels. In order to establish the value of the proposed methodology as a determinant of glaucoma, a larger group of both types of subjects should be investigated. This larger-scale study will be based on recruitment of patients according to a pre-defined protocol, in which patient clinical history and procedures for image acquisition are standardised and described in detail.

Acknowledgement

This work was co-funded by the European Social Fund (75%) and National Resources (25%) - Operational Program for Educational and Vocational Training II (EPEAEK II) and particularly the Program PYTHAGORAS.

References

[1] QUIGLEY H.A. (1993): 'Open Angle Glaucoma', *N Engl J Med.*, **328**, pp. 1097–1106.
[2] SOMMER A. (1996): 'Glaucoma: Facts and Fancies', *Eye*, **10**, pp. 295–301.
[3] SWINDALE N.V., STJEPANOVIC G., CHIN A. and MIKELBERG F.S. (2000): 'Automated Analysis of Normal and Glaucomatous Optic Nerve Head Topography Images', *Investigative Ophthalmology & Visual Science*, **41**, pp. 1730-1742.
[4] SCHUMAN J.S., WOLLSTEIN G., FARRA T., HERTZMARK E., AYDIN A., FUJIMOTO J.G. and PAUNESCU L.A. (2003): 'Comparison of Optic Nerve Head Measurements Obtained by Optical Coherence Tomography and Confocal Scanning Laser Ophthalmoscopy', *American Journal of Ophthalmology*, **135**, pp. 504-512.
[5] CHAN K., TE-WON LEE, SAMPLE P.A., GOLDBAUM M.H., WEINREB R.N., ZANGWILL L.M., SEJNOWSKI T.J. (2002): 'Comparison of Machine Learning and Traditional Classifiers in Glaucoma Diagnosis', *IEEE Trans. Biomedical Engineering*, **49**, pp. 963-974.
[6] MATSOPOULOS G.K., ASVESTAS P.A., MOURAVLIANSKY N.A. and DELIBASIS K.K. (2004): 'Multimodal Registration of Retinal Images Using Self Organizing Maps', *IEEE Trans. Med. Imag.*, **23**, pp. 1557-1563.
[7] PENNEY G.P., WEESE J., LITTLE J.A., DESMEDT P., HILL D.L.G. and HAWKES D.J. (1998): 'A Comparison of Similarity Measures for Use in 2-D–3-D Medical Image Registration', *IEEE Trans. Med. Imag.*, **17**, pp. 586-595.
[8] PUDIL P., NOVOVICOVA J. and KITTLER J. (1994): 'Floating Search Methods in Feature Selection', *Pattern Recognition Letters*, **15**, pp. 1119-1125.
[9] BEZDEK, J. C (1981): 'Pattern Recognition with Fuzzy Objective Function Algorithms', (Plenum Press, New York).

ISSN: 1727-1983